WORLD CONFERENCE ON TIMBER ENGINEERING 2025
BRISBANE, AUSTRALIA
Advancing Timber for the Future Built Environment

Simplified Testing Approach for Predicting Pull-out Strength of Glued-in Rods

Gwang-Ryul Lee[1], Jaewon Oh[2], Kyung-Sun Ahn[3], Min-Jeong Kim[4], Sang-Hyun You[5], Hae Seon Hwang[6], Haegyu Lee[7],Chul-ki Kim[8], Keon-ho Kim[9], Jung-Kwon Oh[10]

ABSTRACT: This study investigates simplified testing approach for predicting the pull-out strength of glued-in rods (GiRs) in Japanese Larch timber. A simplified approach using material parameters (shear strength and mode II fracture energy) derived from epoxy-bonded small wood specimens is suggested to streamline the testing procedure for theoretical model which requires fully-assembled GiR test to determine material parameters. Four empirical models and one theoretical model with simplified approach were evaluated against experimental results from GiR specimens with varying rod diameters (16, 19, and 24 mm) and anchorage lengths (200, 300, and 400 mm). The research demonstrates that two empirical models and theoretical model provide good estimation of pull-out strength of GiRs. However, only the theoretical model with simplified approach maintains prediction accuracy within 10% of experimental values and does not show geometry dependency that is confirmed by statistical analysis. The results indicate that directly measured material properties from small bonded wood specimens can effectively replace parameters that were determined through resource-intensive testing of full GiR assemblies. This methodology offers a practical alternative for engineers designing GiR connections in Japanese Larch and potentially other timber species.

KEYWORDS: Glued-in rod, Pull-out strength, Volkersen's theory, Simplified approach, Validation of models.

[1] Gwang-Ryul Lee, dept. of Agriculture, Forestry and Bioresources, Seoul National University, Seoul, Republic of Korea, qweqweqwer@snu.ac.kr

[2] Jaewon Oh, dept. of Wood Science, University of British Columbia, Vancouver, Canada, jwoh@student.ubc.ca

[3] Kyung-Sun Ahn, dept. of Agriculture, Forestry and Bioresources, Seoul National University, Seoul, Republic of Korea, rudtjs6339@snu.ac.kr

[4] Min-Jeong Kim, dept. of Agriculture, Forestry and Bioresources, Seoul National University, Seoul, Republic of Korea, minjeong.kim@snu.ac.kr

[5] Sang-Hyun Youdept. of Agriculture, Forestry and Bioresources, Seoul National University, Seoul, Republic of Korea, tkdgus2716@snu.ac.kr

[6] Hae Seon Hwang, dept. of Agriculture, Forestry and Bioresources, Seoul National University, Seoul, Republic of Korea, haeseon@snu.ac.kr

[7] Haegyu Lee, dept. of Agriculture, Forestry and Bioresources, Seoul National University, Seoul, Republic of Korea, haegyulee@snu.ac.kr

[8] Chul-ki Kim, Wood Engineering Division, National Institute of Forest Science, Seoul, Republic of Korea, email address or ORCID

[9] Keon-ho Kim, Wood Industry Division, National Institute of Forest Science, Seoul, Republic of Korea, email address or ORCID

[10] Jung-Kwon Oh, dept. of Agriculture, Forestry and Bioresources, Seoul National University, Seoul, Republic of Korea, email address or ORCID

https://doi.org/10.52202/080513-0020

1 – INTRODUCTION

In recent decades, timber have gained significant attention as a sustainable structural material, driven by growing environmental concerns and advancements in manufacturing technology.[1], [2] While traditional timber connections using mechanical fasteners such as nails, bolts, and dowels have been widely utilized, they often suffer from drawbacks including tightening-stresses, initial slippage, limited ductility/dissipation capacity , and vulnerability to fire exposure[2]-[5].

Glued-in Rod (GiR) connections have emerged as an innovative alternative that addresses many of these limitations. These connections, consisting of steel or fiber-reinforced polymer rods bonded into pre-drilled holes with structural adhesives, offer superior load-bearing capacity, enhanced aesthetic appeal and fire resistance through concealed fastening [6]-[8]. Additionally, GiRs enable efficient force transfer while maintaining the structural integrity of timber elements.:

Despite their advantages, accurately predicting the pull-out strength of GiRs remains challenging due to the complex interaction between timber, adhesive, and rod materials. Numerous researchers have proposed empirical models based on experimental results [7] and [9]-[19]. These studies have broadened our knowledge of GiRs, showing that GiRs strength is influenced by multiple factors such as rod diameter, anchorage length, adhesive types and thickness, wood density and loading conditions. However, these models often lack validation across different timber species and geometric configurations. This limitation is intrinsic to empirical approaches, as they may not account for all variability in material properties among different wood species. So validations for various species and configurations are needed to reliably predict the strength of GiRs using these empirical models.

Not only empirical models, but theoretical models were developed [20], [21]. In [20], the authors attempted to explain the behavior of GiR system by incorporating Volkersen theory [22] and non-linear fracture mechanics [23]. They derived quite simple form of equation to predict GiR pull-out strength. Another model [21] suggested the stress distribution equations of shear, normal, radial and hoop stress by solving the governing differential equations. Both approches show good accuracy for evaluating GiR strength, but their practical utility is limited due to the requirments for further efforts to utilize these models. Former model typically requires extensive testing of GiR specimens with varying geometric configurations to determine essential parameters like shear strength of rod-adhesive-timber systems and material property length parameter. Latter one needs sophisticated numerical calculations and computational assistances. Such procedures exhibit a degree of complexity, potentially constraining the practical application of this theoretical models.

The present study has two primary objectives: to validate existing empirical models for predicting pull-out strength of GiRs specifically in Japanese Larch, and to propose a simplified approach to predict the pull-out strength of GiRs using theoritical model in [20]. Rather than conducting tests on full GiR assemblies with different configurations, this research investigates whether the key parameters for prediction model can be derived from tests on epoxy-bonded small wood specimens. This approach, if validated, would significantly streamline the testing process while maintaining prediction accuracy, thereby facilitating the broader adoption of GiR technology in structural applications.

2 – BACKGROUND

2.1 Existing Empirical Models

The analysis and strength prediction of Glued-in Rod (GiR) connections present significant challenges due to the complex interaction between three distinctly different materials: timber, adhesive, and rod. This multi-material system creates complex stress distributions and failure modes that are difficult to model using purely theoretical approaches. So empirical models were mainly proposed rather than theoretical models [24], to predict the pull-out strength of GiRs. These models aim to simplify the complex behavior into practical design equations that can be readily applied by engineers.

The pioneer of this field, Riberholt presented an empirically-derived equation (1) and (2) that incorporated fundamental parameters such as material density, rod diameter, bonded length, and withdrawal parameter [14].

$$R = f_{ws}\rho d_h\sqrt{l}\ (l \geq 200\ mm) \quad (1)$$

$$R = f_{wl}\rho d_h l\ (l \leq 200\ mm) \quad (2)$$

This equation explains that the strength of GiR depends on geometry factors d_h and l, and material properties f_{ws}, f_{wl} and ρ . f_{ws} and f_{wl} are determined by types of adhesives. The value of former factor is 650, 520 N/mm$^{1.5}$ and latter factor is 46, 37 N/mm^2 for non-brittle and brittle adhesives respectively. This model reflect the phenomena that the strength of GiR does not increase proportionally with anchorage length.

In German code DIN 1052, following equation can be founded for withdrawl resistance of GiR [18].

$$R = \pi d_r l f \quad (2)$$

$$f = 4.0\ \text{N/mm}^2 (l \leq 250\ mm) \quad (3)$$

$$f = 5.25 - 0.005l\ (250 < l \leq 500\ mm) \quad (4)$$

According to [25], this equation was investigated as the most prefered model among design methods of GiR. Similar with [14], the influence of anchorage length for improving pull-out strength is reduced as anchorage length increase. This equation does not consider the effect of timber density, while most empirical equations include it as material parameter.

The pre-version of Eurocode [26] presented an empirically-derived equation that incorporated fundamental parameters such as timber density, rod diameter and glued-in length.

$$R = \pi d_h l f \quad (5)$$

$$f = 1.2 \times 10^{-3} \times d_h^{-0.2} \times \rho^{1.5} \quad (6)$$

Unlike (1) and (4) that account for the diminishing effect of increasing bond length on pull-out strength, this model considers the reduction in pull-out strength increasement

https://doi.org/10.52202/080513-0020

as the hole diameter increases. Equation (5) was modified to (7) in [7] to reflect the effect of adhesive's type and thickness.

$$R = \pi l(f d_h + k(d+h)h) \quad (7)$$

$$k = 0.086\ (brittle\ adhesives), \quad (8)$$

$$k = 1.213(ductile\ adhesives) \quad (9)$$

Recently, the draft of prEN 1995-1-1 Eurocode 5 [27] revised the model to address the influence of adhesive thickness or anchorage length. While maintaing the concept of (5) the withdrawal strength f is newly defined to follow EN 17334.

Another models regarding slenderness ratio (λ) as main parameter were developed. In [9], the decreasing nominal shear strength was founded as slenderness ratio increases. Equations (10) and (11) was proposed to account for this behavior.

$$R = \pi d_h l f \quad (10)$$

$$f = 7.8 \times \left(\frac{\lambda}{10}\right)^{-1/3} \times \left(\frac{\rho}{480}\right)^{0.6} \quad (11)$$

The authors limited the validity of this equation only for slenderness ration 7.5-15, and rod diameters 12-20 mm which are typical configurations for practical application.

Similar with (11), according to [11] the withdrawl resistance of GiR can be predicted by incorperation of the geometry factors such as diameter of hole, anchorage length and slenderness ratio, and material properties of timber and joint.

$$R = \pi d_h l f \quad (12)$$

$$f = f_{joint} \frac{\Omega}{\Omega^{2.3}+1} \quad (13)$$

$$\Omega = \frac{\lambda}{f_{timber}} \quad (14)$$

While these approachs provide simplified methods to predict the stiffness of GIRs, they demonstrate notable limitations: as these equations are derived from empirical models, the validations with different test set-up are needed.

2.2 Theoretical models

Equation (15), which is derived from the solution of governing differential equations, was proposed by Hassanieh et al. [21] enabling a more detailed analysis of stress distribution patterns.

$$\tau(r,z) = \frac{d_r((d_w/2)^2 - r^2)}{2r((d_w/2)^2 - (d_r/2+h)^2)} \frac{\partial \sigma}{\partial z} \quad (15)$$

$$\sigma(z) = -\frac{1}{2}\frac{D}{A} + C_1 e^{-w_1 z} + C_2 e^{w_1 z} + C_3 e^{-w_2 z} + C_4 e^{w_2 z} \quad (16)$$

While this approach demonstrates good accuracy, its application is constrained by the requirement for complex numerical methods and computational procedures, rendering it less suitable for practical.

Another theoretical approach founded upon Volkersen's theory and non-linear fracture mechanics(NLFM) was developed in [20].

$$R = \pi d l \tau_f \frac{\tanh\ \omega}{\omega} \quad (17)$$

$$\omega = \sqrt{\frac{l_{geo}}{l_m}} \quad (18)$$

$$l_{geo} = \frac{\pi d_r l^2}{2}\left(\frac{1}{A_r} + \frac{E_r/E_w}{A_w}\right) \quad (19)$$

$$l_m = \frac{E_r G_f}{\tau_f^2} \quad (20)$$

As seen in (17)-(20), the GiR withdrawl resistance is affected by geometry parameters such as cross section area of rod and timber, diameter of rod and anchorage length. Also, the material parameters, e.g. the modulus of elasticity of rod and timber, shear strength and fracture energy of GiR system, are needed to predict GiR capacity.This methodology offers a more comprehensive representation of GiR behavior by accounting for the non-uniform distribution of shear stress along the adhesive line, with stress concentrations at the terminal regions.

This model have been reported to show good accuracy to evaluating the pull-out strength of GiRs in many researches [11], [28], [29]. However, two of material parameters, the shear strength (τ_f) and mode II fracture energy (G_f) should be determined by testing GiR specimens with different configurations. These two factors should be fitted to experimental data of fully assembled GiRs which needs fairly high endeavor both in aspect of time and costs.

2.3 Simplified approach

Glued-in rod connections can experience failure in five distinct zones: 1. rod failure, 2. rod-adhesive interface failure, 3. cohesive failure within the adhesive, 4. adhesive-timber interface failure, and 5. timber failure. These failure modes have been extensively documented in previous studies [10], [20], [30]. Among these, interface failures are generally considered the most critical to avoid in practical engineering applications [31], [32], as they often lead to brittle and unpredictable structural behavior. In GiR connections, this risk can be mitigated by using adhesives with high bonding capacity to both timber and steel, such as epoxy resins. Numerous studies on pull-out tests of epoxy-based GiR connections have consistently reported an absence of rod-adhesive interface failures [10], [20], [29], [33], [34], indicating good adhesion property of epoxy with steel rods.

If we assume that rod-adhesive interface failure does not occur—which can be verified through shear testing of timber-adhesive-steel assemblies—then the pull-out strength of GiR connections would be governed by either rod failure or adhesively bonded wood performance. Since rod failure can be easily calculated as the product of steel tensile strength and rod cross-sectional area, the critical unknown becomes the performance of the bonded wood component.

This understanding forms the foundation of our simplified approach. Rather than determining material factors from complex and resource-intensive tests on fully assembled GiR specimens, this study proposes using data obtained from epoxy-bonded small wood specimens to predict the strength of epoxy-based GiR connections. This approach

https://doi.org/10.52202/080513-0020

is expected to significantly reduces testing complexity while maintaining prediction accuracy, thereby offering a more practical method for engineering applications.

3 – Materials and methods

3.1 Materials

3.1.1 Timber

Japanese larch (*Larix kaempferi*) glued-laminated timber (GLT) was used in this study. The GLT was manufactured under controlled conditions with moisture content maintained below 12% and an average air-dried density of 560.7 kg/m³. Following practical engineering applications, standard material properties according to KS F 3021 [35] were adopted. The material properties of GLT is demostrated in Table 1.

Table 1.Material properties of Japanese Larch.

Property	Value(Mpa)
Bending strength (characteristic)	10
Modulus of elasticity of bending (average)	9000

Table 2. Material properties of HIT-RE 500 V3.

Property (after 7 days)	Value(Mpa)
Tensile strength (average)	49.3
Compressive strength (average)	82.7
Modulus of elasticity (average)	2600

Table 3. Material properties of SS275.

Property	Value(Mpa)
Tensile yield strength (average)	275
Tensile ultimate strength (average)	400
Modulus of elasticity (average)	210,000

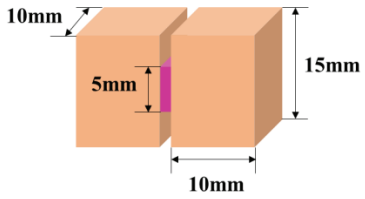

Figure 1. Configuration of bonded wood specimen.

3.1.2 Adhesive

A commercial two-component epoxy adhesive (HIT-RE 500 V3) was selected due to its good bonding properties with both steel and timber. The mechanical properties of this epoxy adhesive, as provided by the manufacturer [36], are listed in Table 2.

3.1.3 Steel Rods

Grade SS275 threaded rods, conforming to KS D 3503 [37], were utilized in this study. These rods were selected for two primary advantages: enhanced bond strength through increased surface area, and facilitation of rapid assembly through nut connections. The material properties of these rods are presented in Table 3.

3.2 Specimen Design and Preparation

3.2.1 Bonded Wood Specimen

To determine the shear strength and fracture energy of adhesively joined wood, 50 specimens that are bonded with two-component epoxy adhesive were prepared. The nominal dimensions and configuration are detailed in Fig. 1. Specimens were cured at 25°C for 3 days.

3.2.2 GiR Specimen

The specimens were designed with dimensions of 150 mm × 150 mm cross-section to ensure compliance with minimum edge distance requirements [38]. By inserting rods into opposite sides of the GLT as shown in Fig. 2, testing under practical pull-pull loading conditions were designed. Key geometric variables included:

- Rod diameters: 16, 19, and 24 mm
- Anchorage lengths: 200, 300, and 400 mm

Three replicate specimens were fabricated for each configuration.

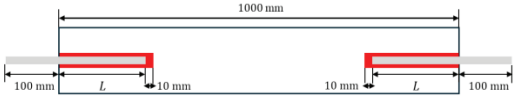

Figure 2. Detailed glued-in rod specimen configurations

The specimen preparation process followed these procedures:

1. Holes were drilled with diameters 2-3 mm larger than the rod diameter
2. Hole depth was extended 10 mm beyond the intended anchorage length
3. Epoxy adhesive was injected into the pre-drilled holes
4. Rods were inserted and centralized using external fixation to prevent eccentricity
5. Specimens were cured according to manufacturer's recommendations

3.3 Testing Setup and Procedure

3.3.1 Bonded Wood Specimen Testing

The concept of test configuration is inspired by [39] and [40]. The main purpose for this experimental setup is to get stable load-displacement curve under shear load. The specimens were fixed by adjusting bolts and lateral supports to avoid the rotation and Mode I failure as illustrated in Fig. 3. Load was implied on the side of fixture near roller at a loading rate of 0.5mm/min. Linear variable displacement transducers (LVDTs) were installed on the load cell and measured the displacement of loading block.

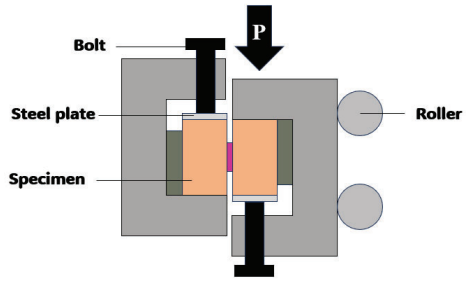

Figure 3. Test set-up configuration of bonded wood specimens

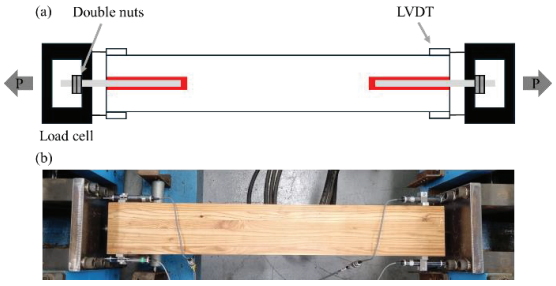

Figure 4. Test set up configuration (a) schematic representation (b) actual setup configuration.

3.3.2 GiR Pull-out Testing

The experimental setup employed a 1000 kN capacity load cell as illustrated in Fig. 4. Based on preliminary tests where single-nut configurations experienced premature failures, double nuts were adopted to ensure proper load transfer and prevent unintended failure modes.

During testing, one side of the specimen was fixed while a tensile force was applied to the opposite rod at a constant loading rate of 2 mm/min. The test continued until a significant load drop occurred, indicating failure. All data including load and displacement measurements were continuously recorded throughout the test.

4 – RESULTS

4.1 Determining shear strength and fracture energy

For loads under 50 N, the inclination of load-displacement curve were assumed same with the average value for $0.1F_{max}$–$0.4F_{max}$. The typical curves are shown in Fig. 5. (a) and Fig. 5. (b), which represents unstable curve and stable curve respectivly. Among 50 specimens, 39 of them showed sudden failure after peak loads and only 11 specimens showed stable curves.

Even though shear failure occurred, some extent loads were observed. The main reasons for these forces are thought of as the unintended resistance owing to non-planar fracture surfaces as illustrated in Fig. 6 . The interference between two blocks might occurred after shear failure of epoxy-bonded specimens. These forces must be eliminated to calculate the mode II fracture energy. The magitude and the onset point of residual forces are needed to accurately remove the residual forces. However, distinguishing it from test curves was impossible in this research. Instead, the amount of minimum forces in each declining curves were substrated from all loads after the peak point. Fig. 7 shows the load-displacement curves including and excluding residual forces. Mode II fracture energy of epoxy-bonded small wood specimens were caculated based on the curves which is not containing residual forces.

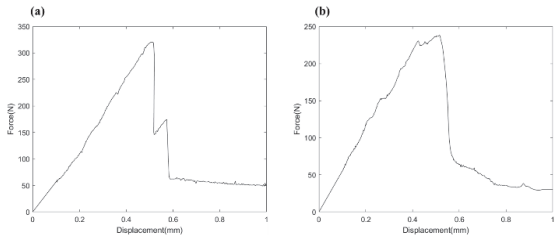

Figure 5. Load-displacement curves of small bonded wood specimens example of (a) unstable curve (b) stable curve.

https://doi.org/10.52202/080513-0020

Figure 6. Non-planar surface of failed specimen.

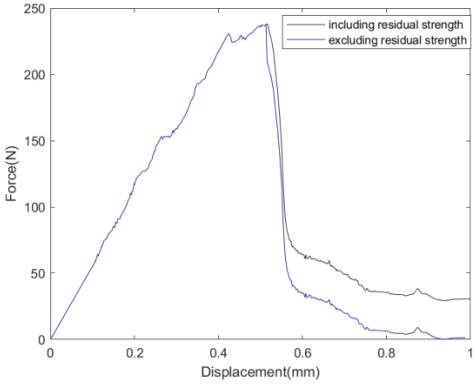

Figure 7. Example of subtracting residual forces.

Mean shear strength is calculated from all specimen, and mean mode II fracture energy is calculated from 11 specimens that showed stable load-displacement curves because evaluating fracture energy based on unstable curves leads to erroneous results [41]-[43]. The result is demonstraed in Table 4. In [20], the authors suggested material parameters τ_f and G_f as 10.5 MPa, 1.89N/mm respectivly for determining average pull-out strength of GiRs when using epoxy adhesives. There are significant difference with this research's test result. Furthermore, according to [44], which provided the basis for in prEN 1995-2 [45], the recommended values for calculating average pull-out load resistance are τ_f = 8.10 MPa and C = 0.0167. However, based on the values in Table 4, τ_f and C were calculated as 7.95 MPa and 0.0197, respectively. This suggests that even when using the similar epoxy-based adhesive, these parameters can vary significantly depending on the timber species and specific adhesive formulation. Therefore, it is questionable whether using identical material parameters for all GiR connections as suggested in prEN 1995-2 [45] is appropriate.

Table 4. Test results of epoxy bonded wood.

Property	Value
Shear strength (average)	7.950 Mpa
Mode II fracture energy (average)	2.066 N/mm

Table 5. Results of GiR pull-out tests.

Specimen Name	P_{test} (kN)	COV (%)
16-200	70.10	5.10
16-300	79.15	12.42
19-200	87.47	6.54
19-300	104.53	6.54
19-400	104.06	2.19
24-300	136.57	6.83
24-400	146.05	15.35

4.2 Pull-out test results

Table 5 shows the average pull-out strength according to different configurations. Results from specimens with nut failure were excluded; all remaining specimens failed due to shear failure in the timber. As demonstrated in many empirical models, the increase in pull-out strength with increasing rod diameter is significant. This is attributed to the larger bond area that allows for better load distribution as diameter increases. In contrast, the effect of increasing anchorage length on strength enhancement is relatively minor compared to that of diameter. Comparing specimens 19-200 and 19-300, despite 1.5 times increase in anchorage length, the strength only increased by approximately 20%. This phenomenon can be explained by Volkersen theory: while increased length provides better load distribution, it simultaneously leads to higher stress concentrations at the end side of the GiR connection.

4.3 Comparison of models

Table 6 shows the mean test results and prediction value caculated by model 1-5. The density of wood was 560.7kg/m3, and in model 4 and 5, the shear strength and mode II fracture energy were 7.95 Mpa and 2.066 N/mm as determined by small epoxy bonded small specimen experiment result.

It seems that empirical models generally overestimate the pull-out resistance of GiRs while theoritical model evaluate the performance conservatively. Among empirical models, model 1 and model 4 showed good accuracy for predicting the strength of GiRs. Model 1 showed prediction to test result ratio(P_{model}/P_{test}) ranging 0.96-1.18, and model 4 showed P_{model}/P_{test} values ranging 0.98-1.17. Model 5 with simplified approach demonstrated good estimation of GiR strength showing P_{model}/P_{test} values from 0.90-1.01.

Although model 1 and 4 well evaluated the strength of GiRs, it seems that there exist geometry dependency on model's accuracy in case of empirical models. For example, as seen in Table 6, model 1-3 show to higher P_{model}/P_{test} ratio value as anchorage length increases while model 4 show opposite tendency. In case of rod diameters, as they increase, the Pmodel/Ptest ratio become smaller in

https://doi.org/10.52202/080513-0020

model 1 and 2, while converse protensity is observed in model 4. To statistically verify the effect of geometry factors on models accuracy, t-tests between all configurations were conducted. The null hypothesis(H_0: $u_1 = u_2$) was rejected if p-value is caculated lower than 0.05. Model 5 was the only one where all configurations maintained the null hypothesis (H_0: $u_1 = u_2$) at the 5% significance level as seen in Table .7. This suggests that while model 1-4 ‘s accuracy might be affected by geometry factors, model 5 shows consistent accuaracy regardless of geometric parameters changes.

Model 5 with simplified approach, not only demonstrates good agreement with experimental results and geometry-independent accuracy but also offers the advantage of using τ_f and G_f values with direct physical meaning rather than data-fitted parameters. Table 8 lists the τ_f and G_f values fitted to this study's test results. Depending on the GiR configurations selected to determine these material factors, τ_f and G_f can vary substantially. In our experimental results, τ_f varied from approximately 6.3 to 11.1 MPa, while G_f ranged from about 2.1 to 4.5 N/mm. Since these values are fitted to experimental results rather than having inherent physical meaning, careful consideration is required when selecting which values to adopt. In contrast, when applying the simplified approach, we could directly use material properties while accurately predicting GiR pull-out performance within a 10% margin of error.

This research has demonstrated the validation of empirical models for predicting GiR strength and presented a streamlined method for determining parameters in the theoretical model. .

5 – CONCLUSION

This research has validated existing empirical and theoretical models for predicting the pull-out strength of glued-in rods in Japanese Larch timber and presented a streamlined method for determining parameters in the theoretical model. The key findings can be summarized as follows:

1. Among the evaluated empirical models, Model 1 [14] and Model 4 [11] demonstrated good accuracy with prediction-to-test ratios ranging from 0.96-1.18 and 0.98-1.17, respectively. However, statistical analysis revealed that these models exhibit geometry-dependent accuracy, limiting their reliability across different configurations.

2. The theoretical model [44] with simplified approach showed consistent prediction accuracy regardless of geometric parameters, with prediction-to-test ratios ranging from 0.90-1.01. Statistical t-tests confirmed the geometry-independent performance of this model at the 5% significance level.

3. The observed variability in fitted material parameters (τ_f: 6.3-11.1 MPa; G_f: 2.1-4.5 N/mm) from different GiR configurations highlights the limitations of using standardized parameters as suggested in some design codes, emphasizing the need for species-specific and adhesive-specific considerations.

Table 6. Comparison of models predicting GiRs pull-out strength.

Specimen Name	**Model 1**[14]		**Model 2** [26]		**Model 3** [9]		**Model 4** [11]		**Model 5*** [20]	
	P_{model} (kN)	P_{model}/P_{test}	P_{model} (kN)	P_{model}/P_{test}	P_{model} (kN)	P_{model}/P_{test}	P_{model} (kN)	P_{model}/P_{test}	P_{model} (kN)	P_{model}/P_{test}
16-200	74.2	1.06	103.5	1.48	89.90	1.28	73.79	1.05	66.26	0.95
16-300	90.9	1.15	155.2	1.96	117.80	1.49	77.62	0.98	79.87	1.01
19-200	86.6	0.99	116.7	1.33	111.06	1.27	95.55	1.09	79.16	0.90
19-300	106.1	1.01	175.0	1.67	145.53	1.39	106.91	1.02	96.32	0.92
19-400	122.5	1.18	233.3	2.24	176.30	1.69	106.92	1.03	104.13	1.00
24-300	131.3	0.96	206.8	1.51	194.77	1.43	159.88	1.17	122.88	0.90
24-400	151.6	1.04	275.7	1.89	235.95	1.62	167.86	1.15	133.58	0.91

* Test results of epoxy-bonded small wood specimen were applied for calculation.

https://doi.org/10.52202/080513-0020

Table .7. Results of t-test between GiR configurations of model 5.

p-value (H_0: $u_1 = u_2$)		u_1 (P_{model}/P_{test})						
		16-200	**16-300**	**19-200**	**19-300**	**19-400**	**24-300**	**24-400**
u_2 (P_{model}/P_{test})	**16-200**	1.0000	0.4588	0.4162	0.6112	0.1394	0.3792	0.7356
	16-300		1.0000	0.2863	0.3502	0.9089	0.2744	0.5546
	19-200			1.0000	0.7528	0.0620	0.9236	0.9194
	19-300				1.0000	0.0920	0.6883	0.9425
	19-400			Sym.		1.0000	0.0614	0.3431
	24-300						1.0000	0.8781
	24-400							1.0000

Table 8. Calculated values of material parameters fitted with test results.

Specimen configurations		u_1 (P_{model}/P_{test})						
		16-200	**16-300**	**19-200**	**19-300**	**19-400**	**24-300**	**24-400**
u_2 (P_{model}/P_{test})	**16-200**	-	τ_f: 10.1770 G_f: 2.1240	*n. d.*	τ_f: 8.7025 G_f: 3.0022	τ_f: 9.7163 G_f: 2.2914	τ_f: 8.4748 G_f: 3.3005	τ_f: 8.8279 G_f: 2.8701
	16-300		-	τ_f: 11.1251 G_f: 2.0533	*n. d.*	τ_f: 8.4754 G_f: 2.4012	*n. d.*	τ_f: 6.2888 G_f: 4.4602
	19-200			-	τ_f: 9.5283 G_f: 2.7154	τ_f: 10.4160 G_f: 2.2567	τ_f: 9.3282 G_f: 2.8785	τ_f: 9.4542 G_f: 2.7720
	19-300				-	*n. d.*	*n. d.*	τ_f: 9.2167 G_f: 2.8049
	19-400			Sym.		-	*n. d.*	*n. d.*
	24-300						-	τ_f: 9.8244 G_f: 2.7289
	24-400							-

While the brittle nature of epoxy adhesives presented challenges in measuring fracture energy, the simplified approach nevertheless demonstrated robust predictive capability. This approach is expected to expand the applicability of the theoritical model, which is regarded as a powerful model for predicting GiR strength.

6 – Nomenclature

R : Pull-out strength of GiR(kN)

ρ : Density of timber

d_h, d_r : Diameter of hole and rod (mm)

l : Anchorage length (mm)

f : Shear strength of material (MPa)

A_c, D_c, w_i, C_i : Coefficients

τ_f : Shear strengh GiR (Mpa)

G_f : Mode II fracture energy of GiR (Mpa)

ω : Coefficient of brittleness ratio

E_r, E_w : Modulus of elasticity of rod and wood (MPa)

A_r, A_w : Cross-section area of rod and wood(mm^2)

7 – REFERENCES

[1] A. A. Firoozi, A. A. Firoozi, D. O. Oyejobi, S. Avudaiappan, and E. S. Flores, “Emerging trends

in sustainable building materials: Technological innovations, enhanced performance, and future directions," *Results in Engineering*, vol. 24, p. 103521, Dec. 2024, doi: 10.1016/j.rineng.2024.103521.

[2] Z. Shu *et al.*, "Reinforced moment-resisting glulam bolted connection with coupled long steel rod with screwheads for modern timber frame structures," *Earthquake Engineering & Structural Dynamics*, vol. 52, no. 4, pp. 845–864, 2023, doi: 10.1002/eqe.3789.

[3] M. Audebert, D. Dhima, A. Bouchaïr, and A. Frangi, "Review of experimental data for timber connections with dowel-type fasteners under standard fire exposure," *Fire Safety Journal*, vol. 107, pp. 217–234, Jul. 2019, doi: 10.1016/j.firesaf.2019.102905.

[4] H. W. Lee, S. S. Jang, and C.-W. Kang, "Evaluation of Withdrawal Resistance of Screw-Type Fasteners Depending on Lead-Hole Size, Grain Direction, Screw Size, Screw Type and Species," *Journal of the Korean Wood Science and Technology*, vol. 49, no. 2, pp. 181–190, Mar. 2021, doi: 10.5658/WOOD.2021.49.2.181.

[5] N. Gattesco and I. Toffolo, "Experimental study on multiple-bolt steel-to-timber tension joints," *Mat. Struct.*, vol. 37, no. 2, pp. 129–138, Mar. 2004, doi: 10.1007/BF02486609.

[6] G. Tlustochowicz, E. Serrano, and R. Steiger, "State-of-the-art review on timber connections with glued-in steel rods," *Mater Struct*, vol. 44, no. 5, pp. 997–1020, Jun. 2011, doi: 10.1617/s11527-010-9682-9.

[7] L. Feligioni, P. Lavisci, G. Duchanois, M. De Ciechi, and P. Spinelli, "Influence of glue rheology and joint thickness on the strength of bonded-in rods," *Holz Roh Werkst*, vol. 61, no. 4, pp. 281–287, Sep. 2003, doi: 10.1007/s00107-003-0387-4.

[8] T. Vallée, T. Tannert, and S. Fecht, "Adhesively bonded connections in the context of timber engineering – A Review," *The Journal of Adhesion*, vol. 93, no. 4, pp. 257–287, Mar. 2017, doi: 10.1080/00218464.2015.1071255.

[9] R. Steiger, E. Gehri, and R. Widmann, "Pull-out strength of axially loaded steel rods bonded in glulam parallel to the grain," *Mater Struct*, vol. 40, no. 1, pp. 69–78, Jan. 2007, doi: 10.1617/s11527-006-9111-2.

[10] A. Rossignon and B. Espion, "Experimental assessment of the pull-out strength of single rods bonded in glulam parallel to the grain," *Holz Roh Werkst*, vol. 66, no. 6, pp. 419–432, Dec. 2008, doi: 10.1007/s00107-008-0263-3.

[11] D. Otero Chans, J. E. Cimadevila, and E. M. Gutiérrez, "Model for predicting the axial strength of joints made with glued-in rods in sawn timber," *Construction and Building Materials*, vol. 24, no. 9, pp. 1773–1778, Sep. 2010, doi: 10.1016/j.conbuildmat.2010.02.010.

[12] The Institution of Structural Engineers, *'Glued joints.' In Manual for the design of timber buildings to Eurocode 5*. United Kingdom: IStructE/TRADA, 2007.

[13] G. Parida, H. Johnsson, and M. Fragiacomo, "Provisions for Ductile Behavior of Timber-to-Steel Connections with Multiple Glued-In Rods," *Journal of Structural Engineering*, vol. 139, no. 9, pp. 1468–1477, Sep. 2013, doi: 10.1061/(ASCE)ST.1943-541X.0000735.

[14] H. Riberholt, "Glued bolts in glulam-proposals for CIB code," Rotterdam (Netherlands), 1988.

[15] T. Y. Li, B. Shan, Y. Xiao, Y. R. Guo, and M. P. Zhang, "Axially loaded single threaded rod glued in glubam joint," *Construction and Building Materials*, vol. 244, p. 118302, May 2020, doi: 10.1016/j.conbuildmat.2020.118302.

[16] S. A and C. Zhou, "Pull-out tests on bond behavior between timber and near-surface-mounted steel bars," *Construction and Building Materials*, vol. 288, p. 122974, Jun. 2021, doi: 10.1016/j.conbuildmat.2021.122974.

[17] C. Binck and A. Frangi, "On stiffness and strength of glued-in rods and threaded rods parallel to the grain," 2024, doi: 10.3929/ETHZ-B-000720943.

[18] Deutsches Institut für Normung (DIN), *DIN 1052: 2008-12. Design of timber structures. General rules and rules for buildings*. Berlin, German: DIN, 2008.

[19] European Committe for Standardization CEN, *Eurocode 5-Design of timber structures-Par 2: Bridges ENV 1995-2:1997*. Brussels, Belgium: CEN, 2003.

[20] P. J. Gustafsson and E. Serrano, "Glued-In Rods for Timber Structures - Development of a Calculation Model," *Division of Structural Mechanics, LTH*, 2001.

[21] A. Hassanieh, H. R. Valipour, M. A. Bradford, and R. Jockwer, "Glued-in-rod timber joints: analytical model and finite element simulation," *Mater Struct*, vol. 51, no. 3, p. 61, Jun. 2018, doi: 10.1617/s11527-018-1189-9.

[22] O. VOLKERSEN, "Die Nietkraftverteilung in zugbeanspruchten Nietverbindungen mit

https://doi.org/10.52202/080513-0020

Konstanten Laschenquerschnitten," *Luftfahrtfor schung*, vol. 15, pp. 41–47, 1938.

[23] P. J. Gustafsson, "ANALYSIS OF GENERALIZED VOLKERSEN-JOINTS IN TERMS OF NON-LINEAR FRACTURE MECHANICS," *Division of Structural Mechanics, LTH*, 1987.

[24] J. L. Jensen, A. Koizumi, T. Sasaki, Y. Tamura, and Y. Iijima, "Axially loaded glued-in hardwood dowels," *Wood Science and Technology*, vol. 35, no. 1, pp. 73–83, Apr. 2001, doi: 10.1007/s002260000076.

[25] M. Stepinac, V. Rajcic, F. Hunger, J.-W. van de Kuilen, R. Tomasi, and E. Serrano, "COMPARISON OF DESIGN RULES FOR GLUED-IN RODS AND DESIGN RULE PROPOSAL FOR IMPLEMENTATION IN EUROPEAN STANDARDS, 46th CIB W18 meeting," *ResearchGate*, 2013.

[26] European Committee for Standardization, *prEN 1995-1-1 Design of timber structures , Part 1-1: General Common rules and rules for buildings*. Brussels, Belgium, 2003.

[27] European Committee for Standardization, *prEN 1995-1-1 Design of timber structures , Part 1-1: General Common rules and rules for buildings*. Brussels, Belgium, 2023.

[28] G. S. Ayansola, T. Tannert, and T. Vallee, "Experimental investigations of glued-in rod connections in CLT," *Construction and Building Materials*, vol. 324, p. 126680, Mar. 2022, doi: 10.1016/j.conbuildmat.2022.126680.

[29] B. Azinović, E. Serrano, M. Kramar, and T. Pazlar, "Experimental investigation of the axial strength of glued-in rods in cross laminated timber," *Mater Struct*, vol. 51, no. 6, p. 143, Oct. 2018, doi: 10.1617/s11527-018-1268-y.

[30] E. Zhao, S. Yu, C. Yang, X. Zhang, F. Wang, and D. Yu, "Pull-out behavior of glulam connections with glued-in rod loaded parallel to the grain," *The Journal of Adhesion*, vol. 0, no. 0, pp. 1–25, doi: 10.1080/00218464.2025.2458558.

[31] A. Shrivastava, "6 - Plastics Part Design and Application," in *Introduction to Plastics Engineering*, A. Shrivastava, Ed., in Plastics Design Library. , William Andrew Publishing, 2018, pp. 179–205. doi: 10.1016/B978-0-323-39500-7.00006-X.

[32] K. Sullivan and K. D. Peterman, "A review of adhesive steel-to-steel connections for use in heavy construction," *Journal of Constructional Steel Research*, vol. 213, p. 108405, Feb. 2024, doi: 10.1016/j.jcsr.2023.108405.

[33] C. Grunwald *et al.*, "Rods glued in engineered hardwood products part I: Experimental results under quasi-static loading," *International Journal of Adhesion and Adhesives*, vol. 90, pp. 163–181, Apr. 2019, doi: 10.1016/j.ijadhadh.2018.05.003.

[34] J. G. Broughton and A. R. Hutchinson, "Pull-out behaviour of steel rods bonded into timber," *Materials and Structures*, vol. 34, 2001.

[35] Korean Standards Association, *KS F 3021: Structural glued laminated timber"*. 2013.

[36] North American Product Technical Guides 22nd ed., *Anchor Fastening Technical Guide*, 2 vols. Hilti Inc., 2022.

[37] Korean Standards Association, *KS D 3503: Rolled steels for general structure*. 2016.

[38] EOTA, *Design of Glued-in Rods for Timber Connections*, vol. TR 070. European Organisation for Technical Assessment (EOTA), 2019.

[39] H. Yoshihara and M. Maruta, "Examination of the block shear fracture test method to measure the Mode-II critical stress intensity factor," *Engineering Fracture Mechanics*, vol. 232, p. 107043, Jun. 2020, doi: 10.1016/j.engfracmech.2020.107043.

[40] Wernersson and P. J. Gustafsson, "THE COMPLETE STRESS-SLIP CURVE OF WOOD-ADHESIVES IN PURE SHEAR," *Division of Structural Mechanics, LTH*, 1987.

[41] I. Smith, E. Landis, and M. Gong, *Fracture and Fatige in Wood*. John Wiley & Sons, 2003.

[42] H. Wernersson, "Fracture Characterization of Wood Adhesive Joints," *Division of Structural Mechanics, LTH*, 1994.

[43] P.-E. Petersson, "Crack growth and develpment of fracture zones in plain concrete and similar materials," *Division of Structural Mechanics, LTH*, 1981.

[44] P. J. Gustafsson and E. Serrano, "Glued-in Rods. Local Bond Line Fracture Properties and a Strength Design Equation," presented at the International Symposium on Wood Based Materials, Wood Composites and Chemistry, 2002. Accessed: Mar. 25, 2025. [Online]. Available: http://lup.lub.lu.se/record/928332

[45] European Committe for Standardization, *prEN 1995-2 Design of timber structures, Part 2: Bridges*. Brussels, Belgium: Final Projcet Team draft. Stage 34, 2003.